Proc. of the 6th Intl. Symposium on Reliability Engineering and Risk Management (6ISRERM)
31 May – 1 June 2018, Singapore
Editor(s) Xudong Qian, Sze Dai Pang, Ghim Ping Raymond Ong, Kok-Kwang Phoon

Multivariate Adaptive Regression Splines Model for Reliability Analysis on Serviceability Limit State of Twin Caverns

Yinrong Fu[2] Anthony T. C. Goh[3] and Wengang Zhang [12]*

[1] *Key Laboratory of New Technology for Construction of Cities in Mountain Area, Chongqing University, Chongqing, China*
[2] *School of Civil Engineering, Chongqing University, Chongqing, China*
[3] *School of Civil and Environmental Engineering, Nanyang Technological University, Singapore*
E-mail: cheungwg@126.com

ABSTRACT

Construction of a new cavern modifies the state of stresses and movements in a zone around the existing cavern, as some degree of interaction between these two caverns takes place. Extensive plane strain finite difference analyses were carried out to examine the deformations induced by excavation of underground twin caverns. Based on the numerical results, a fairly simple nonparametric regression algorithm known as multivariate adaptive regression splines (MARS) model has been used to relate the percent strain to various parameters including the rock quality, the cavern geometries and the in situ stress ratio. Probabilistic assessments on serviceability limit state of twin caverns can be performed using Monte Carlo simulation (MCS) and First-order reliability method (FORM) for comparison. These two reliability approaches give similar and consistent results.

Keywords: reliability analysis, serviceability limit state, critical strain, twin caverns, percent strain, MARS.

1 Introduction

The construction of a new cavern modifies the state of stresses and movements in a zone around the existing cavern. For multiple caverns, the size of this influence zone depends on the ground type, the in situ stress, the cavern span, the width of the pillar separating the caverns, and the excavation sequences. If two adjacent excavations are constructed far apart such that their influence zones do not overlap, then the individual cavern can be considered separately as single caverns and analyzed as such. However, if the influence zones of the two caverns do overlap, some degree of interaction between the two caverns will take place. Interaction of the two caverns will affect the global stability, the state of stress and the deformations around the caverns. The ultimate limit state failure for stress-induced instability was usually assessed in terms of global factor of safety. However, the serviceability limit state, which denotes failure due to excessive movements, should also be considered. Thus an accurate estimation of the deformation induced by cavern excavation is necessary. Considering the uncertainties existing in the design parameters, the calculation on the probability of the cavern deformation exceeding the prescribed limiting value is important.

In this paper, plane strain (PS) finite difference analyses using FLAC^{3D} were performed in which the deformation of the two parallel caverns is investigated. Based on the numerical results, this paper describes the multivariate adaptive regression splines (MARS) models developed for estimating the percent strains ε_t. This study then demonstrates how reliability analysis on the

serviceability limit state of twin caverns can be performed using Monte Carlo simulation (MCS) and First-order reliability method (FORM) to estimate the probability of the cavern deformation exceeding the prescribed limiting value.

2 MARS methodology

Friedman (1991) introduced MARS as a statistical method for fitting the relationship between a set of input variables and dependent responses. It is a nonlinear and nonparametric regression method based on a divide and conquer strategy in which the training data sets are partitioned into separate piecewise linear segments (splines) of differing gradients (slope). For simplicity, MARS details are not provided in this paper.

3 Numerical modeling

3.1 *Assumptions of numerical analysis*

The basic assumptions of numerical analyses in this case are: (i) the study was a 2D PS problem; (ii) the rock material obeyed Mohr-Coulomb (MC) failure criterion; (iii) the caverns are unsupported; (iv) the twin caverns are of equal size, both horse-shoe shaped, with semi-circular roof, the span-to-side wall height ratio (B/H) is 2, and horizontally aligned; (v) the excavation involves six stages: heading, first benching, second benching of the right cavern, followed by heading, first benching, second benching of the left cavern; (vi) the effect of creep was not considered in the analysis.

3.2 *Cross-section layout*

In this study, the PS conditions are enforced by including a thin 1 m slice of material in the longitudinal direction and imposing boundary conditions on the two off-plane surfaces that allow movement vertically but are restrained against displacements normal to these planes. Outer boundaries are located far from the cavern wall. No surface loading above-ground surface is considered. The initial vertical in situ stress σ_v is induced by self-weight of the rock. The physical and geometrical model including the twin caverns and the design variables considered are shown in Fig 1a.

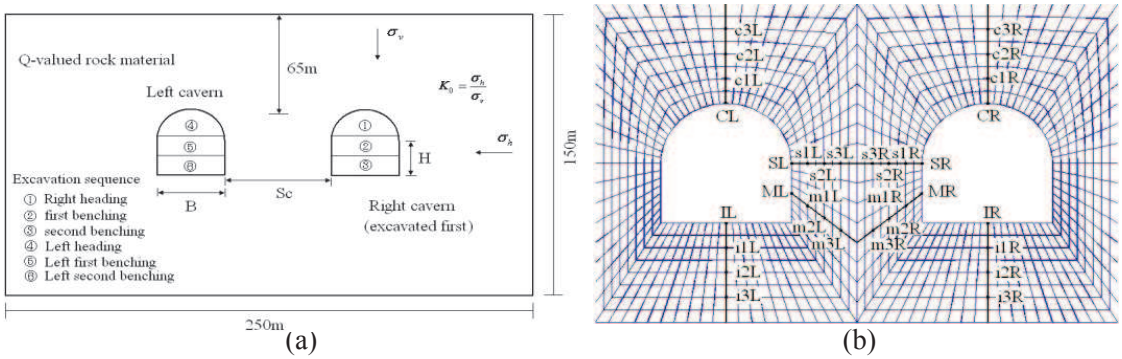

Fig 1. Geometrical model, basic design parameters and details of cavern peripheral nodes

3.3 *Ranges of design parameters*

The main design parameters are listed in Table 1

Table 1. Factors and their values used in parametric studies

Parameter	Description	Values
K_0	In situ stress ratio	0.5, 1, 2
B	Cavern span (m)	10, 20, 30
S_c/B	Ratio of pillar width to cavern span	1, 1.5, 2, 2.5
Q	Tunneling quality index	1, 4, 10, 40, 100

3.4 *Determination of rock mass strength parameters*

In the preliminary stage of an engineering design, the need for an approximate estimate of the rock mass parameters frequently arises. For the numerical analyses carried out in this study, the following equations (Equations 1-6) are adopted for determining the rock mass properties.

$$RMR = 7\ln Q + 36 \quad (Tugrul,\ 1998) \tag{1}$$

$$E_m(GPa) = 10^{(RMR-10)/40} \quad (RMR \le 50) \quad (Serafim\ and\ Pereira,\ 1983) \tag{2}$$

$$E_m(GPa) = 2RMR - 100 \ \ (\text{RMR}>50) \quad (Bieniawski,\ 1978) \tag{3}$$

$$c(MPa) = 0.005(RMR - 1.0) \quad (Bieniawski,\ 1989) \tag{4}$$

$$\phi(^\circ) = 0.5RMR + 4.5 \quad (Bieniawski,\ 1989) \tag{5}$$

$$\sigma_{cm}(MPa) = RMR \quad (Palmstrom,\ 2000) \tag{6}$$

where E_m is the deformation modulus of rock mass, c is the cohesive strength, ϕ is the friction angle, σ_{cm} is the Uniaxial Compressive Strength (*UCS*). Adopting the above empirical equations, the Q value of each category and its corresponding MC rock properties can be determined. For simplicity, density of 2670 kg / m^3 is assumed for rock mass of all the ranges of Q.

3.5 *Determination of the percent strains*

During construction, the displacements of the key points around the cavern like the crown or the invert are usually continuously monitored. These key points include the crown, the springline, the middle side wall, and the invert of the right cavern and of the left cavern, denoted as CR, SR, MR, IR, CL, SL, ML and IL respectively. $u_{\max\_t}$ is defined as $max(u_{CR}, u_{SR}, u_{MR}, u_{IR}, u_{CL}, u_{SL}, u_{ML}, u_{IL})$, in which u_{CR}, u_{SR}, u_{MR}, and u_{IR} are the displacements of peripheral nodes C, S, M and I of the right cavern (firstly excavated), respectively, while u_{CL}, u_{SL}, u_{ML}, and u_{IL} are the displacements of peripheral nodes C, S, M and I of the left cavern, as shown in Fig 1b. The strain value in each of the key points, take ε_{CR} for example, is:

$$\varepsilon_{CR} = \max(\varepsilon_{CR\_c1R}, \varepsilon_{CR\_c2R}, \varepsilon_{CR\_c3R}) \tag{7}$$

in which ε_{CR_ciR} (i=1, 2, 3) is defined as follows (Sakurai 1997, Zhang and Goh 2015, Cui et al. 2017)

$$\varepsilon_{CR\_ciR}(\%) = \frac{u_{CR} - u_{ciR}}{l_{CR\_ciR}} \times 100 \tag{8}$$

where u_{ciR} is the displacement of the corresponding inner node ciR and l_{CR_ciR} is the length between nodes CR and ciR (Fig 1b).
The percent strain of the twin caverns ε_t is the maximum of the strains of the eight key points:

$$\varepsilon_t = \max(\varepsilon_{CR}, \varepsilon_{SR}, \varepsilon_{MR}, \varepsilon_{IR}, \varepsilon_{CL}, \varepsilon_{SL}, \varepsilon_{ML}, \varepsilon_{IL}) \tag{9}$$

As illustrated in Fig 1b, the displacements of 32 nodes are obtained from the numerical analyses from which the percent strain is determined.

4 Modeling Results and Analyses of ε_t

4.1 *Modeling results of ε_t*

Table 2 lists some typical percent strains for brevity.

Table 2. Factors and their values used in parametric studies

Q	K_0	B=20 m				B=30 m			
		0.25	0.5	1	2	0.25	0.5	1	2
10	0.5	0.098	0.047	0.034	0.035	0.160	0.047	0.039	0.049
	1.0	0.094	0.047	0.047	0.046	0.084	0.047	0.051	0.061
	2.0	0.187	0.186	0.183	0.180	0.248	0.173	0.170	0.166
40	0.5	0.021	0.014	0.013	0.013	0.022	0.015	0.015	0.019
	1.0	0.023	0.021	0.021	0.021	0.031	0.021	0.022	0.028
	2.0	0.080	0.077	0.074	0.075	0.106	0.076	0.075	0.077

4.2 *Determination of ε_t using MARS*

MARS model was built to relate ε_t to the parameters Q, S_c/B, K_0 and B, using the data sets from numerical results. Among the 180 design combinations, results of 147 observations are of computational convergence, 109 patterns of which were randomly selected as the training data and the remaining 38 data were used for testing. The optimal MARS model (submodel with the highest R^2 for the testing patterns) adopted 12 BFs of linear spline functions with second-order interaction. The high R^2 of 0.995 for training and 0.994 for testing indicates that the MARS predictions are of high accuracy. For brevity, the ANOVA decomposition of the developed MARS model and the relative importance of the parameters are not detailed here. The conclusion is that ε_t is mainly influenced by Q, followed by K_0. Table 3 lists the BFs of the MARS model for ε_t and their corresponding equations. The interpretable MARS model to predict ε_t is given by

$$\begin{aligned}\varepsilon_{t\_MARS}(\%) &= 0.1 - 0.0093 \times BF1 + 0.046 \times BF2 + 0.14 \times BF3 + 0.074 \times BF4 \\ &-0.0004 \times BF5 + 0.018 \times BF6 + 0.025 \times BF7 + 0.0007 \times BF8 + 0.0013 \times BF9 \\ &+0.0084 \times BF10 + 0.0018 \times BF11 + 0.0043 \times BF12\end{aligned} \tag{10}$$

Table 3. BFs and corresponding equations of MARS model for ε_t

BFs	Equation	BFs	Equation
BF1	max(0, Q - 4)	BF7	BF2×max(0, 2.5 - S_c/B)
BF2	max(0, 4 - Q)	BF8	max(0, Q - 40)
BF3	BF2×max(0, K_0 -1)	BF9	max(0, 40 - Q) ×max(0, 2 - S_c/B)
BF4	max(0, K_0 - 1)	BF10	max(0, Q - 10)
BF5	BF4×max(0, Q -10)	BF11	max(0, 40 - Q) ×max(0, K_0 - 1)
BF6	BF4×max(0, 10 - Q)	BF12	max(0, 1.5 - S_c/B) ×max(0, B - 20)

5 Probabilistic Assessment on Serviceability Limit State

Design line, which is based on an additional 50% of the elastic strain ε_e (Meguid and Rowe 2006), is suggested to limit the induced strains to within tolerable limits. Strains between the limits bounded by the elastic and design lines are considered to be acceptable and will not cause instability at those four locations. Based on this design methodology, numerical trials are performed to derive the elastic responses under combinations of Q, K_0 and B. The elastic responses are obtained through FDM analyses with the rock mass assumed as linear elastic. For brevity, the results of elastic response are skipped. The strain value of the design line ε_d is 1.5 times that of the elastic strain ε_e. The allowable strains are summarized in Table 4 for the cases of Q=1, 4, 10, 40, and 100, respectively.

Table 4. Suggested ε_c for various Q values

Q	1	4	10	40	100
ε_c (%)	0.082-0.227	0.047-0.131	0.033-0.090	0.019-0.052	0.013-0.036

The serviceability limit state function based on the MARS model is given by

$$g(\mathbf{x}) = \varepsilon_c - \varepsilon_{t\_MARS} \tag{11}$$

The expressions of BFs in this equation can be found in Table 3. Reliability assessment of the percent strain using MCS is shown in Fig 2a and FORM in Fig 2b for comparison. In view that there are sometimes the over- or under-excavations, all the four parameters are assumed as in-deterministic in this study.

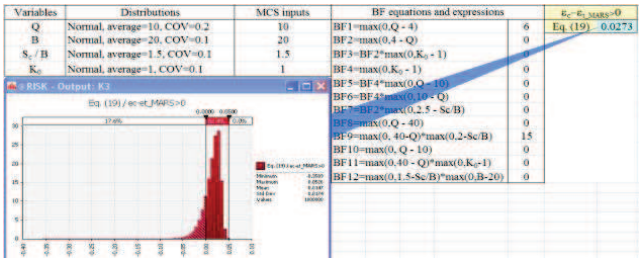

(a)

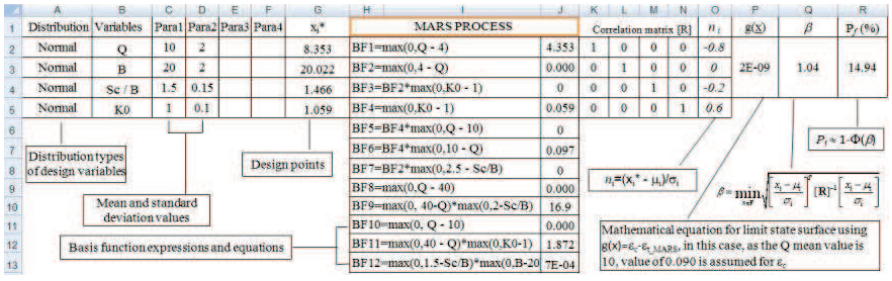

(b)

Fig 2. Implementation of MARS model into: (a) MCS, and (b) FORM for reliability analyses

A comparison of the P_f obtained using the FORM_MARS and the MCS_MARS methods in Fig 3 shows that the FORM_MARS gives similar and consistent results with MCS_MARS.

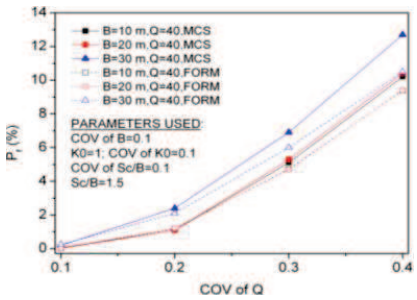

Fig 3. Comparison of P_f of SLS from FORM_MARS and MCS_MARS

6 Conclusions

This paper considered the serviceability limit state of twin caverns. The dependent response is the percent strain ε_t. MARS model relating the percent strain ε_t to the influencing factor is developed and is also adopted as the serviceability criterion. The threshold strain values are determined through the elastic and design line methodology proposed by Meguid and Rowe (2006). Probabilistic assessments on SLS were performed using the MARS percent strain model. Both the FORM_MARS and MCS_MARS reliability methods give similar and consistent results.

References

Journal Papers

Aksoy, C. O., Ozacar, V., Kantarci, O., An example of estimating rock mass deformation around an underground opening using numerical modeling. International Journal of Rock Mechanics and Mining Sciences 47(2), 272-278,2010.

Basarir, H., Engineering geological studies and tunnel support design at Sulakyurt dam site, Turkey. Engineering Geology 86(4), 225-237, 2006.

Bieniawski, Z. T., Determining rock mass deformability: experience from case histories. International Journal of Rock Mechanics and Mining Sciences & Geomechanics Abstracts 15, 237-247, 1978.

Cui L, Zheng JJ, Dong YK, Zhang B, Wang A. 2017. Prediction of critical strains and critical support pressures for circular tunnel excavated in strain-softening rock mass. Engineering Geology 224: 43-61.

Friedman, J. H., Multivariate adaptive regression splines. The Annals of Statistics 19, 1-141, 1991.

Hoek, E., Brown, E.T., Practical estimates of rock mass strength. International Journal of Rock Mechanics and Mining Sciences 34(8), 1165-1186, 1997.

Meguid, M. A., Rowe, R. K., Stability and D-shaped tunnels in a Mohr-Coulomb material under anisotropic stress conditions, Canadian Geotechnical Journal (43), 273-281, 2006.

Serafim, J. L., Pereira, J. P., Considerations of the geomechanics classification of Bieniawski. Proc. of the International Symposium on Engineering Geology and Underground Construction, Lisbon, A.A. Balkema, Rotterdam, the Netherlands, 1, 1133-1142, 1983.

Tugrul, A., The application of rock mass classification systems to underground excavation in weak lime stone, Ataturk dam. Turkey Engineering Geology 50, 337-345, 1998.

Zhang WG, Goh ATC., Regression models for estimating ultimate and serviceability limit states of underground rock caverns. Engineering Geology 188: 68-76, 2015.

Books

Barton, N., Løset, F., Lien, R., Lunde, J., Application of the Q-system in design decisions. In Subsurface Space, New York: Pergamon 2, 553-561, 1980.

Bieniawski, Z. T., Engineering Rock Mass Classifications. John Wiley and Sons, New York, 1989.

Proceedings Papers

Palmstrom, A., On classification systems. Proceedings GeoEng2000, Melbourne, 2000.

Sakurai S., Strength parameters of rocks determined from back analysis of measured displacements", In: First Asian Rock Mechanics Symposium, ISRM. Seoul, pp. 95-99, 1997.